REMPI mass spectrum of the OH radical in the gas phase

R. Forster, H. Hippler, K. Hoyermann, G. Rohde
Institut für Physikalische Chemie der Universität Göttingen, Tammannstrasse 6, W-3400 Göttingen, Germany

and

Lawrence B. Harding
Theoretical Chemistry Group, Chemistry Division, Argonne National Laboratory, Argonne, IL 60439, USA

Received 16 July 1991

The resonance-enhanced multiphoton ionization (REMPI) of the OH radical in the gas phase was studied using an isothermal discharge–flow reactor for the production of OH radicals ($H+NO_2 \rightarrow OH+NO$), tunable laser light from an excimer-pumped dye laser, and a time-of-flight (TOF) mass spectrometer. A mass-resolved REMPI spectrum was found in the wavelength region of 290–310 nm, which is assigned to a (3+1) ionization process. An ab initio quantum-chemical calculation predicts the Rydberg state, verified by the experiment.

1. Introduction

The OH radical in the gas phase plays a central role in many reactive systems of basic and technical interest like hydrocarbon oxidation and air chemistry. The detection by spectroscopic methods and the analysis of the spectra involving low-lying energetic states are well developed. Besides the identification by absorption, emission and resonance-absorption spectroscopy, an increasing application of laser-based methods is to be noticed: laser-induced fluorescence (LIF) [1], laser-induced saturation fluorescence [2], laser-induced predissociation fluorescence (LIPF) [3], laser magnetic-resonance spectroscopy (LMR) [4], and resonance-enhanced multiphoton ionization/photoelectron spectroscopy (REMPI-PES) [5]. (The few references are chosen for a basic description and a recent application and do not reflect the priority; for a review, see also ref. [6].) Here we report on the multiphoton ionization of the OH radical and the detection by mass spectroscopy (REMPI-MS). The REMPI method can be a useful addition to the methods available as it is very sensitive via single-ion detection and as it might be specific if there exists a radical specific wavelength for ionization, a low spectral interference with other species present and an ion-mass selection. A high sensitivity for the detection of radicals is often observed via the ionization of a Rydberg state [7]. The increasing capabilities of precise ab initio quantum-chemical calculations and the prediction of energetically high-lying electronic states (as Rydberg states of the OH radicals) encouraged this joint project of the theoretical prediction and the experimental verification, whose result is presented in this Letter.

2. Experimental

The experimental arrangement as shown in fig. 1 has been described partly in a previous paper [8]. It is a combination of an isothermal discharge–flow reactor coupled to the ion source of a TOF mass spectrometer for a laser-induced multiphoton ionization and a mass-selective ion detection by a timed transient digitizer and/or a boxcar integrator. The OH radicals are produced in the isothermal flow reactor by the reaction $H+NO_2 \rightarrow NO+OH$, where the H atoms are formed by the microwave discharge of highly diluted H_2/He mixtures and the NO_2 (diluted with

0009-2614/91/$ 03.50

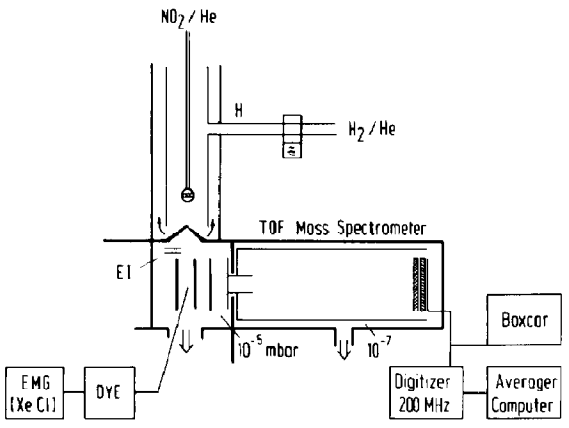

Fig. 1. Experimental arrangement.

He/Ar) is admixed into the main flow by a movable inlet probe. Typical experimental conditions for the OH source are: pressure in the flow reactor around 1 mbar, linear flow velocity around 30 m/s, mole fraction of OH < 0.3 mol% (i.e. $[OH] = 1.4 \times 10^{-10}$ mol/cm^3, 7×10^{13} molecule/cm^3), temperature around 295 K.

By the expansion through a conical nozzle the OH radicals pass the ion source of the mass spectrometer (surrounding pressure 10^{-5}–10^{-6} mbar). Multiphoton ionization is achieved by focusing the laser light into the center of the ion source. An excimer laser (Lambda Physik LPX 205 iCC; XeCl) pumps the dye laser (Lambda Physik FL 2002) for the SHG (KDP, FL 30) of laser light in the region 290–312 nm. (Dye: rhodamin 6G, rhodamin B.) The OH^+ ions are extracted in several stages and injected into the drift tube for the detection by a double-stage microchannel plate detector. The mass spectrum is either recorded by a transient digitizer and averaged over 50–500 cycles (LeCroy SA 3500) or by a gated boxcar integrator/averager (SRS), the latter especially for the measurements of the wavelength dependence of the OH^+ ion production (see fig. 3).

3. Results and discussion

3.1. Theoretical predictions

The theoretical study consists of multi-reference, singles and doubles, configuration-interaction calculations. The calculations employ a polarized valence double-zeta basis set [9] augmented with two sets of diffuse s functions ($\alpha = 0.064$ and 0.024) and two sets of diffuse p functions ($\alpha = 0.052$ and 0.017) on the oxygen atom. The diffuse functions were optimized to describe the 3s and 3p Rydberg states of atomic oxygen. For the ground state of the neutral and the positive ion, the reference wavefunctions consist of a full-valence complete active space (CAS) (6 or 7 electrons and 5 orbitals), with the orbitals self-consistently optimized for each of these states. The Rydberg states were obtained from CI calculations employing the orbitals from the positive ion. For these states, the active orbitals include the five valence orbitals from the ion together with the two lowest sigma virtuals (3s and $3p_z$) and the lowest π virtuals ($3p_x$ and $3p_y$). The reference wavefunction then consists of a CAS amongst these active orbitals with the restriction that only one electron is allowed into the four Rydberg functions. The calculations were carried out with the COLUMBUS program package [10] on a Cray-XMP computer. The calculated excitation energies are summarized in table 1.

The calculated ionization potential is too low by approximately 0.5 eV due to the use of a relatively small basis set. It is expected that the errors in the Rydberg excitation energies should be quite similar to that in the ionization potential. These predictions are shown in parentheses in table 1. The good agreement between the calculated and observed excitation energies for the D state validates the theoretical model used here.

The state of most interest in the present context is the $3\,^2\Pi$ state. The present calculations agree with earlier predictions [12] that this state exhibits a sharp avoided crossing with the $2\,^2\Pi$ state as the character of the state changes from $(\pi \rightarrow 3p_\pi)$ to $(\sigma \rightarrow 3s)$. This crossing occurs very close to the minimum of the $3\,^2\Pi$ state. The calculated potential curves are given in fig. 2.

3.2. Measurements

3.2.1. Mass spectrum

In fig. 3a, the mass spectrum of the OH radical at the wavelength 293.2 nm is shown. At this wavelength, an additional fragment ion (O^+) at $m/e = 16$

Table 1
Calculated and experimental excitation energies (eV) of OH. For the Rydberg states, the numbers in parentheses are obtained by combining the calculated binding energy of the state relative to the $^3\Sigma^-$ ion and the observed ionization potential

State	Character	Vertical excitation energy	Adiabatic excitation energy (T_e)	Exp. [a] (T_e)
$1\,^2\Sigma^+$ (A state)	$(\sigma\rightarrow\pi)$	4.27	4.24	4.05
$2\,^2\Sigma^+$ (B state)	$(\pi\rightarrow 3s)$	11.26 (11.8)	b)	8.65
$1\,^2\Sigma^-$	$(\pi\rightarrow 3s)$	7.87 (8.4)	–	
$2\,^2\Sigma^-$ (D state)	$(\pi\rightarrow 3p_z)$	9.90 (10.4)	9.82 (10.3)	10.18
$1\,^2\Delta$	$(\pi\rightarrow 3s)$	9.86 (10.4)	–	
$2\,^2\Pi$	$(\pi\rightarrow 3p_\pi)$	10.01 (10.5)	9.94 (10.4)	
$3\,^2\Pi$	$(\pi\rightarrow 3p_\pi)$ and $(\sigma\rightarrow 3s)$	12.08 (12.6)	10.49 (11.0)	
$1\,^3\Sigma^-$ (ion)	$(\pi\rightarrow\infty)$	12.49	12.43	12.9–13.0

[a] Ref. [11].
[b] The B state should have a long-range minimum which was not examined in this study.

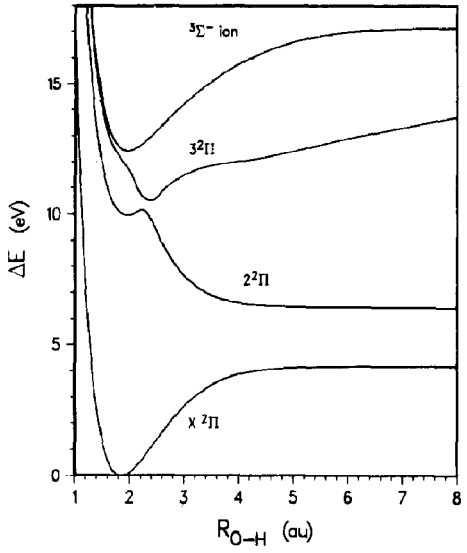

Fig. 2. Potential curves of the OH radical. (For the assignment of the states see table 1.)

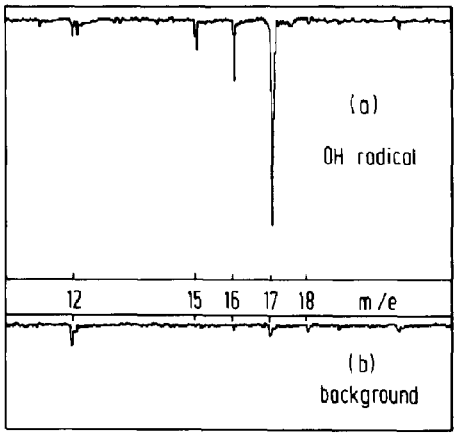

Fig. 3. REMPI mass spectrum of the OH radical at a wavelength of 293.2 nm: (a) OH radical as produced by the reaction $H+NO_2\rightarrow OH+NO$; (b) background (absence of the OH radical, discharge for the production of H atoms off, H_2O added).

is observed, whose intensity is lower at other wavelengths. (The signal at $m/e=12$ is due to residual hydrocarbons present despite the use of turbo-molecular pumps in the experimental setup. The signal at $m/e=15$ at this wavelength is due to an unidentified impurity produced by the microwave discharge, present, too, in the absence of reactants H/H_2/NO_2/NO.) The wavelength-specific detection of OH radicals is obvious by comparing the mass spectra in figs. 3a and 3b, where in fig. 3b no multiphoton ionization of H_2O is observed. (Under the conditions of fig. 3b, microwave discharge off, only He/H_2/NO_2 and added H_2O are present.)

3.2.2. Wavelength dependence: spectrum of the OH radicals

The multiphoton ionization spectrum of the OH radicals was observed in the wavelength region 290.0–310.0 nm as shown in figs. 4a–4d. The calibration of the wavelength scale was performed by comparison with the lines of a Ne lamp. Typical laser repetition rates were 5–10 Hz at an average pulse energy of 2 mJ and a spectral resolution of 0.198 cm^{-1}. The gate time of the boxcar averager was 70 μs with

J.A. Silver, W.L. Dimpfl, J.H. Brophy and J.L. Kinsey, J. Chem. Phys. 65 (1976) 1811;
J.E. Goldsmith, Appl. Opt. 29 (1990) 4841.

[2] K. Kohse-Höinghaus, R. Heidenreich and T. Just, 20th Symposium (International) on Combustion (The Combustion Institute, Pittsburgh, 1984) p. 1177.

[3] P. Andresen, A. Barth, W. Groger, H.W. Lulf, G. Meijer and J.J. terMeulen, Appl. Opt. 27 (1988) 365.

[4] K.M. Evenson, J.S. Wells and H.E. Radford, Phys. Rev. Letters 25 (1970) 199;
P.B. Davies, W. Hack, A.W. Preuss and F. Temps, Chem. Phys. Letters 64 (1979) 94.

[5] E. de Beer, M.P. Koopmans, C.A. de Lange, W.A. Chupka and Y. Wang, private communication (September 1990).

[6] A.C. Eckbreth, 18th Symposium (International) on Combustion (The Combustion Institute, Pittsburgh, 1981) p. 1471;
W. Hack, Intern. Rev. Phys. Chem. 4 (1985) 165.

[7] J.W. Hudgens, in: Advances in multi-photon processes and spectroscopy, ed. S.H. Lin (World Scientific, Singapore, 1987).

[8] P. Heinemann-Fiedler and K. Hoyermann, Ber. Bunsenges. Physik. Chem. 92 (1988) 1472.

[9] T.H. Dunning Jr., J. Chem. Phys. 90 (1989) 1007.

[10] R. Shepard, I. Shavitt, R.M. Pitzer, D.C. Comeau, M. Pepper, H. Lischka, P.G. Szalay, R. Ahlrichs, F.B. Brown and J.-G. Zhao, Intern. J. Quantum Chem. Symp. 22 (1988) 149.

[11] K.P. Huber and G. Herzberg, Molecular spectra and molecular structure, Vol. 4. Constants of diatomic molecules (Van Nostrand Reinhold, New York, 1979) p. 508.

[12] E.F. van Dishoeck and A. Dalgarno, J. Chem. Phys. 79 (1983) 873.

[13] R.W.B. Pearse and A.G. Gaydon, The identification of moleculear spectra, 4th Ed. (Chapman and Hall, London, 1976) p. 264.

[14] S.G. Lias, J.E. Bartmess, J.F. Liebman, J.L. Holmes, Rh.D. Levin and W.G. Mallard, J. Phys. Chem. Ref. Data 17, Suppl. 1 (1988).

[15] J.A. Stephens and V. McKoy, Phys. Rev. Letters 62 (1989) 889.